Journal of Cluster Science, Vol. 18, No. 1, March 2007 (© 2007)
DOI: 10.1007/s10876-007-0111-3

^{27}Al NMR Study of the Metal Cluster Compound $Al_{50}C_{120}H_{180}$*

D. Bono,[1] J. Hartig,[2] M. Huber,[2] H. Schnöckel,[2] and L. J. deJongh[1,3]

Received September 13, 2006; accepted November 14, 2006; published online March 28, 2007

We present an ^{27}Al NMR study of the metal cluster compound $Al_{50}Cp^*_{12}$ which is composed of (identical) Al_{50} clusters, each surrounded by a Cp* ligand shell, and arranged in a crystalline 3D array (here Cp* = pentamethylcyclopentadienyl = $C_5(CH_3)_5$). The compound is found to be non-conducting, the nuclear spin-lattice relaxation in the temperature range 100–300 K being predominantly due to reorientational motions of the Cp* rings. These lead to a pronounced maximum in the relaxation rate at $T \sim 170$ K, corresponding to an activation energy of about 850 K. Data for the related compound $Al_4Cp^*_4$, containing very much smaller Al_4 clusters are also presented. A comparison is drawn with the quadrupolar relaxation recently observed for the non-conducting fraction of Ga_{84} molecules in the metal cluster compound $Ga_{84}[N(SiMe_3)_2]_{20}$-$Li_6Br_2(thf)_{20}$·2toluene.

KEY WORDS: metal clusters; NMR; quadrupolar relaxation.

INTRODUCTION

The synthesis of molecular metal cluster compounds presents an attractive chemical route for the generation of self-organized nanostructures composed of 3D ordered arrays of identical metal nanoparticles embedded in a dielectric matrix [1–9]. These stoichiometric compounds form macromolec-

*It is our pleasure to dedicate this paper to our colleague professor Günter Schmid at the occasion of his 70th birthday.

[1]Kamerlingh Onnes Laboratory, Leiden University, P.O. Box 95042300RA, Leiden, The Netherlands.
[2]Institut für Anorganische Chemie, Universität Karlsruhe, 76128, Karlsruhe, Germany.
[3]To whom correspondence should be addressed. E-mail: jongh@physics.leidenuniv.nl

ular solids, in which the cores of the macromolecules can be seen as minute pieces (clusters) of metals, surrounded by shells of ligand molecules, which pacify the bonds left open at the surfaces of the metal cores in order to prevent the thermodynamically favored formation of the bulk metal. The cluster-molecules can be ions, forming ionic compounds together with suitable counterions. Or they can be electrically neutral and crystallize into molecular solids through intermolecular Van der Waals bonds. The ''self-organized 3D nanostructures'' produced by the crystallization process can thus be viewed as arrays of identical metal nanoparticles, embedded in the dielectric matrix formed by ligands and, if present, the counterions. In the overwhelming majority of compounds studied so far, electron transfer between clusters proved negligible, the materials being electrically insulating (only hopping-type conductivity was observed [10, 11]). Accordingly, the experiments were probing single-particle properties at the nano-scale, such as surface effects, quantum-size effects and the size-induced metal–nonmetal transition [12–15].

On the other hand, on basis of the strong similarity with (super)conducting molecular crystals like the alkali-doped fullerenes, it has been suggested [8] that under suitable conditions metal cluster compounds could likewise show metallic conductivity (or even superconductivity) due to intermolecular charge transfer. Indeed, recently compelling evidence was obtained from ^{69,71}Ga-NMR studies [16] for the occurrence of band-type conductivity by intercluster charge transfer in crystallographically fully characterized Ga_{84} cluster compounds, composed of giant Ga_{84} cluster molecules that display mixed-valency properties [17, 18]. In addition bulk superconductivity has been observed for these compounds [19–21] below a transition temperature $T_c \approx 8$ K, much higher in fact than known for bulk -Ga metal ($T_c \approx 1$ K).

At present the detailed mechanisms underlying the intercluster charge transfer responsible for the metallic properties in the Ga_{84} compounds are still unknown. In what way are these compounds different from the great majority of analogous ionic molecular cluster compounds found to be insulating? To answer such questions is crucial when one attempts to find other examples. In the present note we report a ^{27}Al NMR study on $Al_{50}Cp^*_{12}$, which is another giant molecular cluster compound recently discovered [22], where Cp* = pentamethylcyclopentadienyl = $C_5(CH_3)_5$. Writing the chemical formula as $Al_{50}C_{120}H_{180}$ underlines the fact that the molecular structure can be briefly described as a pseudofullerene shell of 60 carbon atoms and 60 methyl groups, protecting a cluster core of 50 Al atoms. In the following we denote the material by Al_{50} in a shorthand notation. Since the cluster molecules are neutral and the HOMO/LUMO-derived gap of the molecular crystal can be expected to be large, electrical

conductivity would not be expected in this material, as confirmed by the experiments described below. Nuclear relaxation in this material turns out to be predominantly determined by the quadrupolar relaxation channel. As will be shown below, the relaxation in Al_{50} is drastically affected by hindered reorientational motions of the Cp* groups, which form a "surface layer" around the Al_{50} cores. For comparative reasons, we also performed ^{27}Al NMR experiments on the related cluster compound $Al_4Cp^*_4$ (denoted by Al_4), having a much smaller metal core but with the same ligand [23].

SAMPLE DESCRIPTION

Full descriptions of the molecular structures of Al_4 and Al_{50} can be found in Refs. [23] and [22].

The unit cell of the Al_4 sample is triclinic (space group P1), with $a = 1.08326(5)$ nm, $b = 1.09742(3)$ nm, $c = 1.81366(5)$ nm, $\alpha = 82.95°$, $\beta = 82.11°$ and $\gamma = 66.86°$ (at 200 K). It contains two Al_4 clusters located at (0.29639,0.22294,0.25032) and (0.70361, 0.77704, 0.74968). The diameter of one cluster is of order 0.7 nm whereas the distance between the center of two nearest neighboring clusters is 1.356 nm.

In the case of Al_{50}, the cell parameters are $a = 1.93530(39)$ nm, $b = 2.15890(43)$ nm, $c = 2.18180(44)$ nm in an orthorhombic lattice system (Pnnn), with two clusters per unit cell, whose centers are at position (3/4, 1/4, 1/4) and (1/4, 3/4, 3/4). The diameter of the clusters is 1.5 nm whereas the distance between two nearest neighboring clusters is about 1.8 nm. They consist of a central Al_8 core, surrounded by an icosidodecahedral Al_{30} shell, and an outer icosahedral Al_{12} shell. Each Al atom of this external shell is linked to a Cp* molecule.

In Fig. 1a and b, we show a representation of the whole molecules, with the CH_3 groups at the periphery included. The measurements described below were taken on a single crystal of Al_{50} ($\sim$1 mg) and on powder samples ($\sim$15 mg) of both materials.

EXPERIMENTAL RESULTS

The ^{27}Al (spin $I = 5/2$, gyromagnetic ratio $\gamma/2\pi \approx 11.094$ MHz/T) NMR experiments were performed in an external magnetic field $B_0 \approx 9.3$ T in the temperature range 70 K $\leq T \leq$ 300 K. We used either a conventional $\pi/2$–τ–π pulse sequence (measuring the spin-echo), or a free induction decay signal.

In a powder sample of Al_4, one main ^{27}Al line is measured, as expected from the single site, as shown in Fig. 2. It is centered at 102.883 Mhz, corresponding to a chemical shift of about -90 ppm, which is close to the

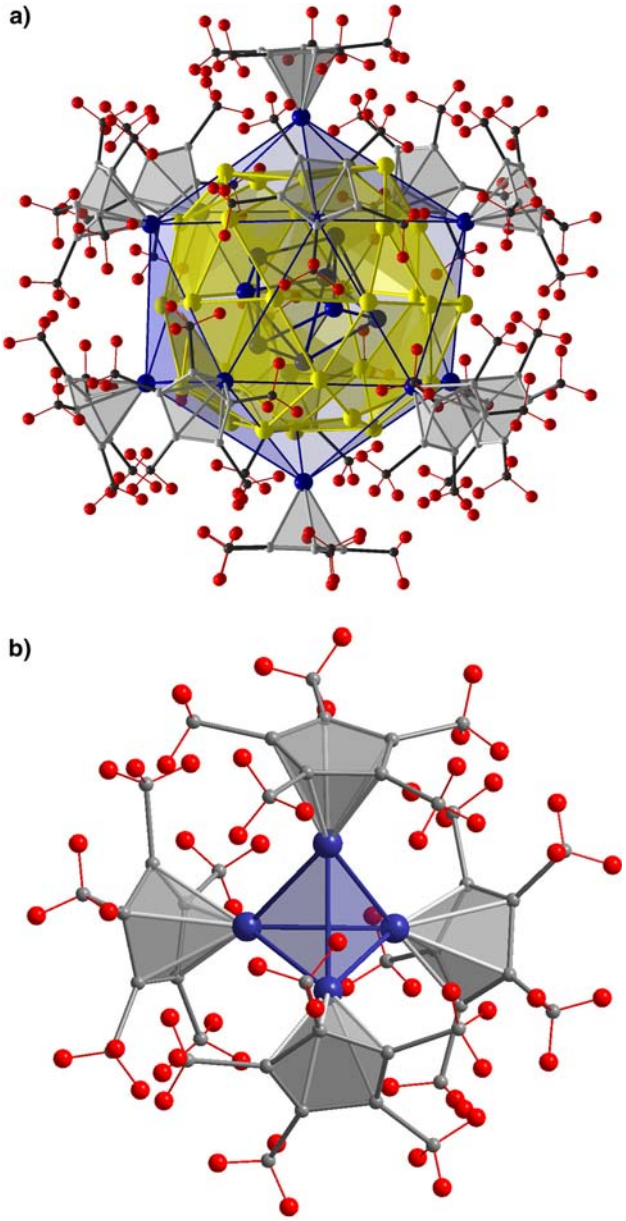

Fig. 1. (a) Structure of an $Al_{50}Cp^*_{12}$ cluster. The Al_{50} core (Al_8 (blue)-Al_{38} (yellow)-Al_{12} (blue) shells) and the ligands ($12C_5(CH_3)_5$ rings) are shown. (b) $Al_4Cp^*_4$ molecule. The aluminum atoms are in blue. In both molecules the carbon atoms are in grey and/or black, the hydrogen atoms in red.

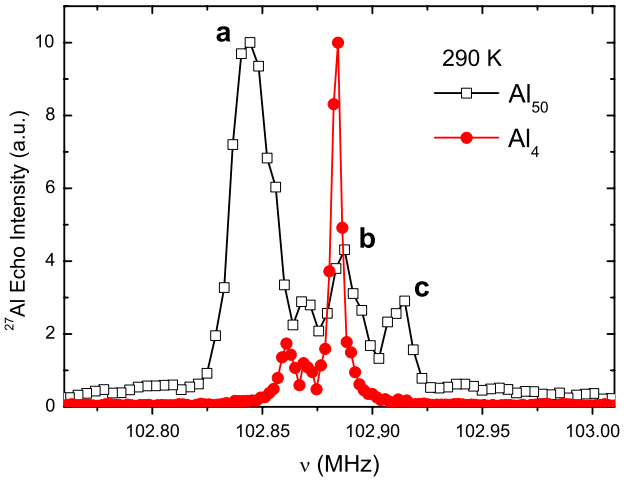

Fig. 2. ^{27}Al spectra in the powder of Al_4 and in the Al_{50} single crystal (SC) at 290 K.

value −80.8 ppm measured in solution [23]. We remind that in Al metal, the Knight shift is 1640(10) ppm (corresponding to $\nu \approx 103.07$ MHz here) [24]. In addition to this main line, two small signals can be discerned at frequencies of about 102.86 and 102.87 MHz. As will be seen below, also in

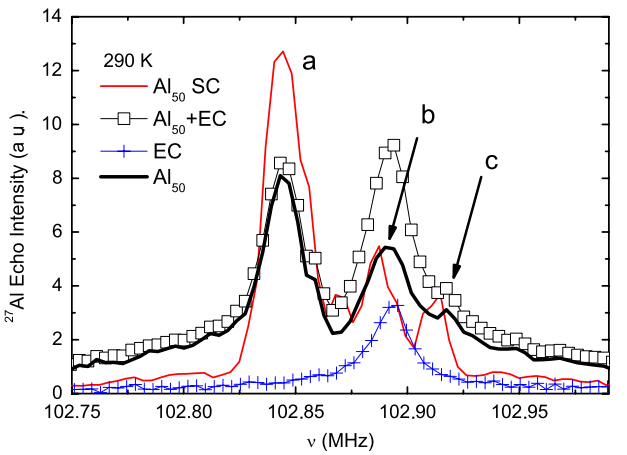

Fig. 3. Comparison of the ^{27}Al spectra measured in Al_{50} with the SC (thin line) and the powder sample (□). The symbols + show the sample holder (SH) signal, only present for the powder sample measurement. The thick line is a subtraction ('□'–'+'), corresponding to the sample signal, which is in good agreement with the SC case.

the powder and single crystal spectra of Al_{50} (Figs. 2 and 3) two small signals can be discerned at these same frequencies. We suspect them to originate from an Al compound present in the catalyst used in the polymerization of the material (PCTFE – polychlortrifluorethene) from which the sample holders were machined. In view of the extreme reactivity of the samples, we cannot fully exclude as another possible origin the presence of small amounts of impurity phases to have developed at the sample surfaces, in spite of all our precautions. At any rate, we shall not consider these spurious signals in the discussion of the spectra given below.

Concerning Al_{50}, the spectrum measured on the single crystal at room temperature displays three different ^{27}Al lines, that we label *a*, *b*, *c* in Fig. 2, respectively centered at 102.845(5) MHz, 102.887(5) MHz and 102.913(5) Mhz. Their respective weights (shifts) are of order 65% (−460 ppm), 23% (−50 ppm) and 12% (200 ppm) [25]. Considering that there are three different Al moieties, in proportion 60% (Al_{30}), 24% (Al_{12}) and 16% (Al_8), with respective theoretical shifts in solution of −372.9, 108.5 and −269.8 ppm [22], we attribute the line *a* to the Al_{30} shells. Since there is some uncertainty in the intensities, and since the observed shifts correspond quite well to the theoretical values, we attribute the line *b* to the Al_8 and the line *c* to Al_{12}. In view of the small size of the single crystal, relaxation studies were performed on a powder sample. Both spectra are compared in Fig. 3. In the course of the powder sample measurements, it became clear that part of the line centered at 102.894 MHz came from a coupling of the NMR coil in this experiment to an (unknown) Al component in the environment of the probe. This became clear by measuring the signal of the empty coil (EC) in the same configuration (+ symbols in Fig. 3). By isolating the NMR probe sufficiently, this spurious contribution could be avoided in the other experiments. Up till now we were not able to measure the spectrum of the powder with another sample holder since the powder sample became deteriorated after the experiment. However, the subtraction of the empty holder signal in case of the powder experiment yields a similar spectrum as for the single crystal (in which case we checked that the EC signal was not present). In any case, it is clear from Fig. 3 that the line *a*, representing 60% of the Al sites, can be well isolated in the spectrum. The lines *b* and *c* can also be distinguished. The signal below ~102.8 MHz and above ~102.93 MHz is probably due to the usual quadrupolar powder pattern [26], although we did not manage to measure any satellite on the single crystal.

In both Al_4 and Al_{50} the ^{27}Al spectra are found to be temperature-independent, as illustrated in Fig. 4, where the intensity of each spectrum has been multiplied by the temperature value in order to account for the paramagnetic susceptibility of the nuclear spins. It indicates among others

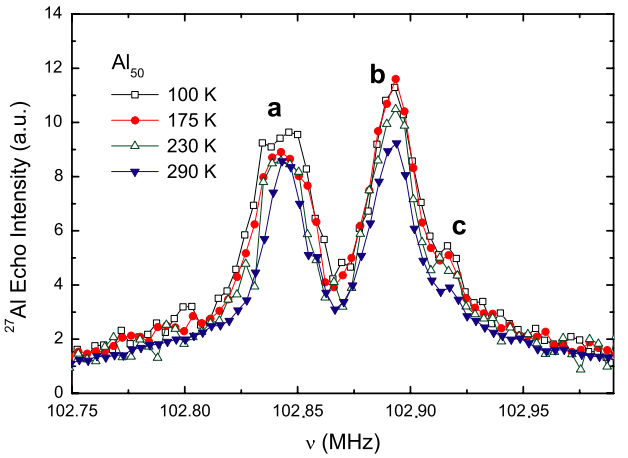

Fig. 4. ^{27}Al spectra measured with the powder sample for several temperatures (the spurious phase is not subtracted).

that the transverse relaxation time T_2 is temperature independent, as expected from dipole-dipole (flip-flop) interactions [27], We measured its value at 290 K in both samples, by changing the time τ between the two rf pulses and measuring the intensity of the spin echo, the center of which is at a time $t \approx 2\tau + 1.32\, t_\pi$ after the end of the π/2 pulse (t_π is the duration of the π-pulse) [28]. The results are displayed in Fig. 5. We used an exponential

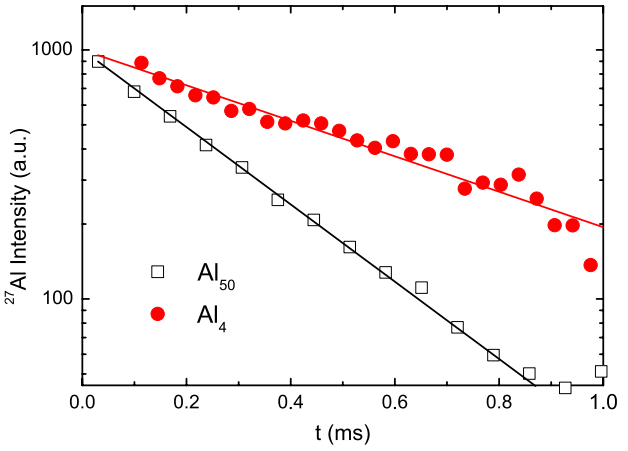

Fig. 5. Spin echo intensity versus the time t for both samples Al_4 and Al_{50} at room temperature (line a in the case of Al_{50}). The lines are single exponential fits.

decay to fit the data (lines in Fig. 5) and find $T_2 = 610 \pm 50$ μs and $T_2 = 260 \pm 10$ μs, respectively in Al_4 and in Al_{50}.

When the transverse relaxation time T_2 is due to flip-flop processes in a powder sample, the T_2 is given by the equation

$$T_2^{-1} = \left[\frac{3}{10}\gamma^4\mu_0^2\hbar^2 I(I+1)\sum_k \frac{1}{r_k^6}\right]^{1/2}, \tag{1}$$

where the sum is taken over the nuclear like-spin sites (in our case, ^{27}Al sites). Flip-flop processes between ^{27}Al nuclei in the same Al_{50} cluster would yield $T_2 \leq 3$ μs, given the distance of order 280 pm between two nearest neighbors. This is much faster than the measured value. However, as proposed for the magnetic cluster compound Mn_{12}-acetate [29], it is clear that such *intra*cluster flip-flops may not equilibriate the nuclear magnetization over the whole crystal. For that, the (much) slower *inter*cluster nuclear spin flips have to be considered. Taking for r_k the distance between the centers of the cluster molecules of the crystal, the calculation yields $T_2 \approx 170$ μs and $T_2 \approx 230$ μs, respectively in Al_4 and in Al_{50}. The latter value is in good agreement with the measurement. The Al_4 value is about three times smaller than the measurement. This may be due to the fact that the line is much narrower (see Fig. 2), leaving less possibility for spectral diffusion than in Al_{50}.

We also measured the temperature dependence of the longitudinal relaxation time (T_1). For this, we applied a π-pulse before waiting for a time t and measuring the echo. The resulting magnetization recovery curves were fitted using the function suited for the central transition ($-1/2 \leftrightarrow 1/2$) of nuclear spins $I = 5/2$, i.e., [30],

$$\frac{M(t)}{M(0)} = 1 - \frac{2}{35}\exp(-[t/T_1]^\alpha) - \frac{16}{45}\exp(-[6t/T_1]^\alpha) - \frac{100}{23}\exp(-[15t/T_1]^\alpha). \tag{2}$$

Here the stretching exponent α is a parameter that takes into account the possible distribution of T_1 over the sites in the sample. Notice that this formula is in principle valid only in the case of purely *magnetic* fluctuations. In the absence of those, the relaxation of the nuclei will be due to the fluctuations of the transverse components of the electric field gradient, through the $\Delta m = 1, 2$ relaxation transition probabilities W_1 and W_2 [27]. In this case the relaxation is called *quadrupolar* and the exact fitting functions, much more complex, are given by Suter *et al.* in Ref. [30]. However, the same authors point out that even in case of strong

quadrupolar fluctuations (and vanishing magnetic ones), a fit with Eq. (2) will give the good order of magnitude for T_1 [30], and can therefore be used in most cases. Magnetization recovery curves are displayed in Fig. 6, with a normalized abscissa. It shows that the shape of $M(t)/M(0)$ is temperature independent. The presence of several ^{27}Al inequivalent sites in the cluster probably yields a distribution of T_1, usually responsible for $\alpha < 1$. The fit yields $\alpha = 0.65(5)$ in the case of Al_{50} (see the line in Fig. 6).

The temperature dependence of T_1^{-1} is reported in Fig. 7. Contrary to Ga_{84}, the Korringa law, i.e., $T_1^{-1} = aT$, characteristic of a metal, is not followed. The dashed line in Fig. 7 sketches T_1^{-1} expected for ^{27}Al in metallic Al ($a = 0.54(2)$ s^{-1} K^{-1}) [31]. *Al_{50} is therefore clearly non-metallic*. The conduction electron spins usually offer the most efficient relaxation channel in metals. Here, their absence implies a relatively small relaxation rate T_1^{-1}, due fully to quadrupolar fluctuations. As seen in Fig. 7, T_1^{-1} increases when the temperature is decreased from room temperature, displays a maximum around 175 K and decreases below. The relaxation rate is much lower in Al_4 which means that the quadrupolar fluctuations are also smaller.

DISCUSSION

A pronounced maximum in the temperature dependence of the nuclear spin relaxation rate, as measured here for Al_{50}, was already reported in

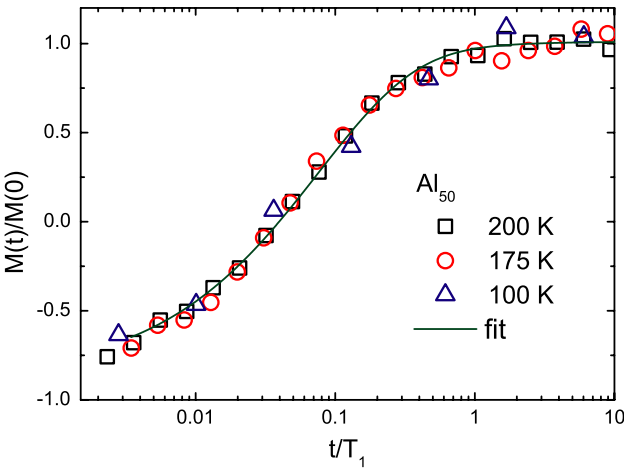

Fig. 6. Magnetization recovery curves for Al_{50} for three temperatures. The line is a fit with Eq. 2 and $\alpha = 0.65$. The abcissa is normalized by the respective T_1 values obtained with this fit.

several compounds, where molecular motions in a multiwell potential frame are responsible for this quadrupolar relaxation behavior [32–36]. Here, either the rotation of CH_3 groups or reorientational motions of the Cp* rings can be responsible for these motions.

Using the equation [33]

$$T_1^{-1} = A\tau/\left[1 + (\omega\tau)^2\right], \tag{3}$$

with $\tau = \tau_0 \exp(E_{\text{eff}}/T)$, we find $\tau_0 = 10 \pm 1 \times 10^{-12}$ s and $E_{\text{eff}} = 850 \pm 20$ K. The function may be slightly different, in particular due to some possible high temperature effects accounting for the levelling off above 250 K (e.g., $\propto T^2$, like in Ref. [34]), that we cannot determine within our temperature range. Although this would yield a better fit, the parameters τ_0 and E_{eff} would remain of the same order of magnitude.

The value obtained for the activation energy appears a bit too high to be attributed to rotational tunneling of the CH_3 groups. For CH_3 rotors appearing in benzene derivatives values for E_{eff} are typically in the range of 10–50 meV (100–500 K), see the recent compilation of Prager and Heidemann [35]. On the other hand, barriers for ring re-orientations are typically of the order of a few tens of kJ/mol (~1000 K) [36]. It appears therefore more plausible to attribute the observed dynamics to reorientations of the Cp* rings.

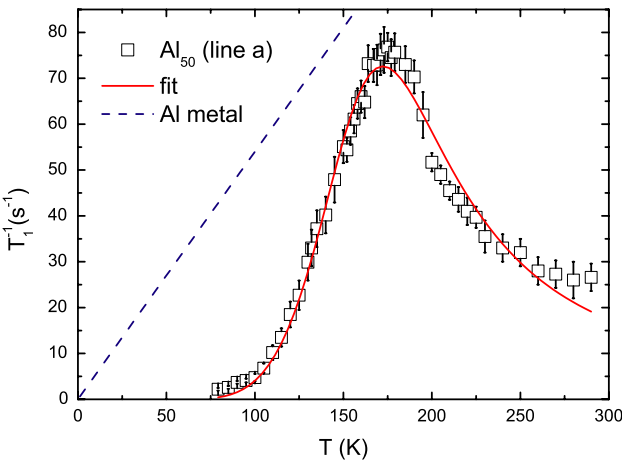

Fig. 7 Temperature dependence of the quadrupolar relaxation rate $1/T_1$, measured on the line *a* for Al_{50}. The dashed line sketches the Korringa law expected in Al metal for ^{27}Al. The continuous line is a fit with Eq. 3.

Interestingly, the small cluster compound $Al_4Cp^*_4$ does not show any evidence for hindered rotational motions in the investigated temperature range. Apparently, the rotational barriers for ring reorientations are much higher than for the $Al_{50}Cp^*_{12}$, probably due to a denser packing in the smaller cluster compound.

In the investigated temperature range the values for the rate found for the Al_4 compound are a factor of 50 lower than for Al_{50}. They are also lower by an order of magnitude than the ^{71}Ga quadrupolar relaxation rates recently observed [20] for the non-conducting fraction of Ga_{84} molecules in the cluster compound $Ga_{84}[N(SiMe_3)_2]_{20}Li_6Br_2$ $(thf)_{20}$-2toluene. A compilation of the relaxation data observed for these three systems is made in Fig. 8. We note that, also for the Ga_{84} compound the temperature dependence of the rate as found above 100 K is much steeper ($\sim T^4$) than expected for phonon-induced quadrupolar relaxation ($\sim T^2$). This suggests the contribution of another relaxation channel in this range, similar as found here for the Al_{50} compound.

In conclusion we can state that the here reported studies demonstrate the profound influences which molecular motions in the ligand shells may have on the nuclear relaxation of metal atoms in the inner cores of molecular metal cluster compounds. Obviously, proton NMR experiments on the ligand molecules themselves should provide valuable complementary information to the present study. We hope that such data will become available in a near future.

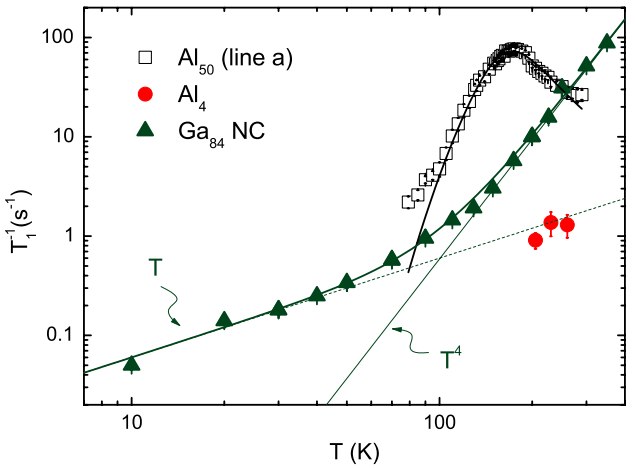

Fig. 8 Comparison of the nuclear relaxation rates in Al_{50}, Al_4 and in the non-conducting (NC) fraction of the Ga_{84} compounds.

ACKNOWLEDGMENTS

This work is part of the research program of the "Stichting FOM" and is partially funded by the EC-RTN "QuEMolNa" (No. MRTN-CT-2003-504880), the EC-Network of Excellence "MAGMANet" (No. 515767-2), and the DFG-Centre for Functional Nanostructures (Karlsruhe).

REFERENCES

1. L. J. de Jongh, in *Organic and Inorganic Low Dimensional Crystalline Materials* (Plenum Press, 1987), p. 231, proceedings Nato Advance Research Workshop, 3rd-8th May, Minorca, Spain.
2. G. Schmid (1992). *Chem. Rev.* **92**, 1709.
3. G. Schmid (1998). *J. Chem. Soc., Dalton Trans.* p. 1077.
4. G. Schmid and L. F. Chi (1998). *Adv. Mater.* **10**, 515.
5. A. Ecker, E. Weckert, and H. Schnöckel (1997). *Nature* **387**, 379.
6. A. Schnepf and H. Schnöckel (2001). *Angew. Chem. Int. Ed.* **41**, 3532.
7. G. Schmid, *Clusters and Colloids* (VCH Weinheim, 1994).
8. L. J. de Jongh, in *Physics and Chemistry of Metal Cluster Compounds* (Kluwer, Dordrecht, 1994), Chap. 1.
9. P. Braunstein, L. A. Oro, and P. Raithby (eds.), *Metal Clusters in Chemistry* (Wiley-VCH and Weinheim, 1999), Vol. I–III.
10. J. A. Reedijk, L. J. Adriaanse, H. B. Brom, and L. J. Jonghde (1998). *Phys. Rev. B* **57**, R15116.
11. M. P. J. Staverenvan, H. B. Brom, and L. J. Jonghde (1991). *Phys. Rep.* **208**, 1.
12. F. M. Mulder, T. A. Stegink, R. C. Thiel, L. J. Jonghde, and G. Schmid (1994). *Nature* **367**, 716.
13. Y. Volokitin, J. Sinzig, L. J. Jonghde, G. Schmid, M. N. Vargaftik, and I. I. Moiseev (1996). *Nature* **384**, 621.
14. F. C. Fritschij, H. B. Brom, L. J. Jonghde, and G. Schmid (1999). *Phys. Rev. Lett.* **82**, 2167.
15. P. M. Paulus, A. Goossens, R. C. Thiel, A. M. Kraanvan der, G. Schmid, and L. J. Jonghde (2001). *Phys. Rev. B* **64**, 205418.
16. O. N. Bakharev, N. Zelders, H. B. Brom, A. Schnepf, H. Schnöckel, and L. J. Jonghde (2003). *Eur. Phys. J. D* **24**, 101.
17. A. Schnepf and H. Schnöckel (2001). *Angew. Chem. Int. Ed.* **40**, 711.
18. A. Schnepf, B. Jee, H. Schnöckel, E. Weckert, A. Meents, D. Lubbert, E. Herrling, and B. Pilawa (2003). *Inorg. Chem.* **42**, 7731.
19. J. Hagel, M. T. Kelemen, G. Fischer, B. Pilawa, J. Wosnitza, E. Dormann, H. Löhneysenvon, A. Schnepf, H. Schnöckel, U. Neisel *et al (2002)*. *J. Low Temp. Phys.* ***129, 133.***
20. O. Bakharev, D. Bono, H. B. Brom, A. Schnepf, H. Schnöckel, and L. J. Jonghde (2006). *Phys. Rev. Lett.* **96**, 117002.
21. D. Bono, A. Schnepf, J. Hartig, H. Schnöckel, G. J. Nieuwenhuys, A. Amato, and L. J. Jonghde (2006). *Phys. Rev. Lett.* **97**, 077601.
22. J. Vollet, J. R. Hartig, and H. Schnöckel (2004). *Angew. Chem. Int. Ed.* **43**, 3186.
23. C. Dohmeier, C. Robl, M. Tacke, and H. Schnöckel (1991). *Angew. Chem. Int. Ed.* **30**, 564.
24. P. L. Sagalyn and J. A. Hofmann (1962). *Phys. Rev.* **127**, 68.
25. The unshifted position for ^{27}Al is $\nu_0 = \gamma B_0/2\pi \approx 102.89$ MHz.

26. J. F. Baugher, P. C. Taylor, T. Oja, and P. J. Bray (1969). *J. Chem. Phys.* **50**, 4914.
27. A. Abragam, *Principles of Nuclear Magnetism* (Clarendon Press-Oxford, 1961).
28. C. Slichter, *Principles of Magnetic Resonance*, 3rd edn. (Springer-Verlag, 1989).
29. A. Morello, O. N. Bakharev, H. B. Brom, R. Sessoli, and L. J. Jonghde (2004). *Phys. Rev. Lett.* **93**, 197202.
30. A. Suter, M. Mali, J. Roos, and D. Brinkmann (1998). *J. Phys.: Condens. Matter.* **10**, 5977.
31. J. J. Spokas and C. P. Slichter (1959). *Phys. Rev.* **113**, 1462.
32. C. Dimitropoulos, J. Pelzl, and F. Borsa (1990). *Phys. Rev. B* **41**, 3914.
33. F. Cordero, R. Cantelli, M. Corti, A. Campana, and A. Rigamonti (1999). *Phys. Rev. B* **59**, 12078.
34. S. Torre and A. Rigamonti (1987). *Phys. Rev. B* **36**, 8274.
35. M. Prager and A. Heidemann (1997). *Chem. Rev.* **97**, 2933.
36. D. Braga (1992). *Chem. Rev.* **92**, 633.